Applied Surface Science Advances 4 (2021) 100083

Contents lists available at ScienceDirect

Applied Surface Science Advances

journal homepage: www.elsevier.com/locate/apsadv

Analysis the effect of TiO_2 addition on sintering, physical mechanical behavior of porcelain insulating material

Niraj Singh Mehta [a,*], Subhashish Dey [b,*], Vaibhav Singh [c], Manas R. Majhi [c]

[a] Department of Electronics and Communication, Roorkee College of Engineering, Roorkee, Uttarakhand, India
[b] Environmental Engineering Department, Rajiv Gandhi Proudyogiki Vishwavidyalaya, Bhopal, India
[c] Department of Ceramic Engineering, Indian Institute of Technology (BHU), UP, India

ARTICLE INFO

Keywords:
Porcelain insulating material
High sintering temperature
Density and physic-mechanical properties

ABSTRACT

The present study is aimed to develop a high strength porcelain insulating material from locally available low cost raw porcelain materials by reinforcement of TiO_2 (0 to 10 in wt.%) as a substitute replacing ZrO_2 in the base porcelain material composition. Base porcelain composition was prepared from the mixture of kaolin, ball clay, quartz, feldspar. Pellets were prepared by applying a constant pressure of 170 MPa using isostatic hydraulic press with holding for a period of 10 min. Different characterizations techniques such as; X-ray diffraction (XRD) and scanning electron microscopy (SEM) used to evaluate the structural and micro structural changes, respectively by increasing the concentration of TiO_2 (0–10 wt.%) and decreasing ZrO_2 (10–0 wt.%) concentration at the base composition of porcelain composition. The measurement of mechanical strength and physical behavior of TiO_2 and ZrO_2 were analyzed for all the samples prepared with different compositions at sintering temperature (1250 and 1350 °C) with soaking period of 2 h. The base porcelain composition with 5 wt.% TiO_2-doped concentration yields the better physical and mechanical strength. The investigated TiO_2 based porcelain material using in refractory and high-temperature insulating applications where severe thermal shock with high mechanical features are required.

1. Introduction

Porcelain is one of the most important composite ceramics; mainly it is a composition of kaolin, ball clay, feldspar and quartz. Kaolin is the primary material from which porcelain is made, even though clay minerals might account for only a small proportion of the whole. The composition of porcelain is highly variable, but the clay mineral kaolinite is often a raw material [1–3]. The role of clay is to provide plasticity that maintain its shape and also act as binder to other component when it is not fired [4–6]. It is fabricate when it is sintered in between 1200 °C and 1400 °C. Porcelain is a ceramic material that having unique properties such as good thermal stability, high mechanical strength, high dielectric constant, low electrical conductivity and high resistivity which differentiate it from other ceramic composite material [7–10].

Over the last decade, the development pace of worldwide production of porcelain made material are expanding in everyday life like stoneware tiles, building construction, photovoltaic supports and insulators than other ceramic items due to its excellent mechanical properties and prevalent stylish execution. It is also environment friendly as it does not cause pollution and it is cheaper as it is easily available [11–12]. Porcelain and other ceramic materials have numerous applications in engineering, particularly ceramic engineering. Porcelain is an excellent insulating material used at high voltage, especially in outdoor, such as for high-voltage cables, brushings of power transformers, insulation of high frequency antennas etc. Porcelain can be utilized as a structure material, generally as tiles or huge rectangular panels [13–15]. Modern porcelain tiles are generally produced by various perceived international standards and definitions. On account of its durability, resistance to rust and impermeability, glazed porcelain has been used for individual cleanliness since from last of the seventeenth century. After that, some problem always occurs on the porcelain made material to achieve a required goal during in continuation of long service [16–18]. In this research work, TiO_2 substitutes as a doping material in alumina-zirconia based composition to influencing the microstructure and mechanical properties of resultant base porcelain material. TiO_2 work as nucleating agent which controlling the crystallization of different crystalline phases [19, 20]. A small additions of titanium oxide increases the secondary mullite and due to this improve the density and micro structural characteristics of the resultant composition. The aim of this work is to examine the role played by the increasing amounts of TiO_2 concen-

* Corresponding authors.
E-mail addresses: nsmehta.rs.cer13@iitbhu.ac.in (N.S. Mehta), subhashish.dey.civ11@itbhu.ac.in (S. Dey), vaibhavsingh.rs.cer17@itbhu.ac.in (V. Singh), mrmajhi.cer@iitbhu.ac.in (M.R. Majhi).

https://doi.org/10.1016/j.apsadv.2021.100083
Received 21 November 2020; Received in revised form 20 February 2021; Accepted 3 March 2021

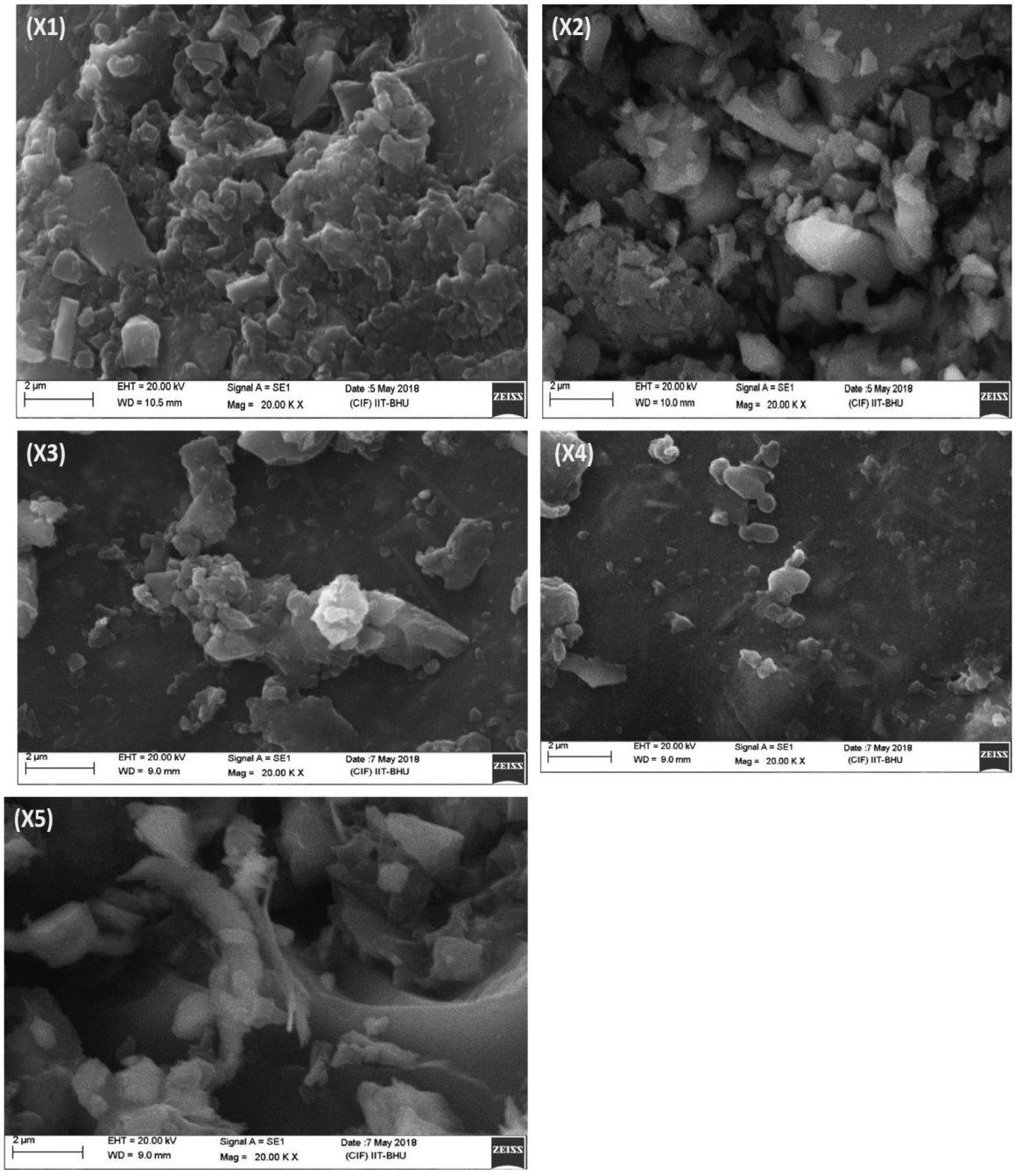

Fig. 1. SEM micrograph of different composition of porcelain material sintered at 1250 °C.

tration on micro structural characterization in base porcelain material. A second objective is to analysis TiO_2 effect on bending or flexural as well as compressive strength in porcelain material [21–24].

2. Experimental techniques

The base composition of raw porcelain material is prepared using 40 wt.% of kaolin, 25 wt.% of ball clay, 15 wt.% of feldspar and 10 wt.% Quartz with varying the (10–0) wt.% of ZrO_2 and TiO_2 (0–10%) wt.% contents. The fabrication process of different sample is shown in the Table 1. This raw material are hygroscopic in nature, so they are placed in an oven at a temperature of 110 ± 5 °C for 24 h to remove the moisture content from it. Afterwards, the powder materials were crushed and grinded up to 150 µm sieve individually before mixing to form the base composition. The powder material is poured on the sieve of 150 µm size to ensure the uniformity of particle size. The said composition in

Table 1
Formulation of alumina zirconia based porcelain composition.

Samples	Taken in weight%					
	Kaolin	Ball Clay	Feldspar	Quartz	ZrO_2	TiO_2
X1	40	25	15	10	10	0
X2	40	25	15	10	7.5	2.5
X3	40	25	15	10	5	5
X4	40	25	15	10	2.5	7.5
X5	40	25	15	10	0	10

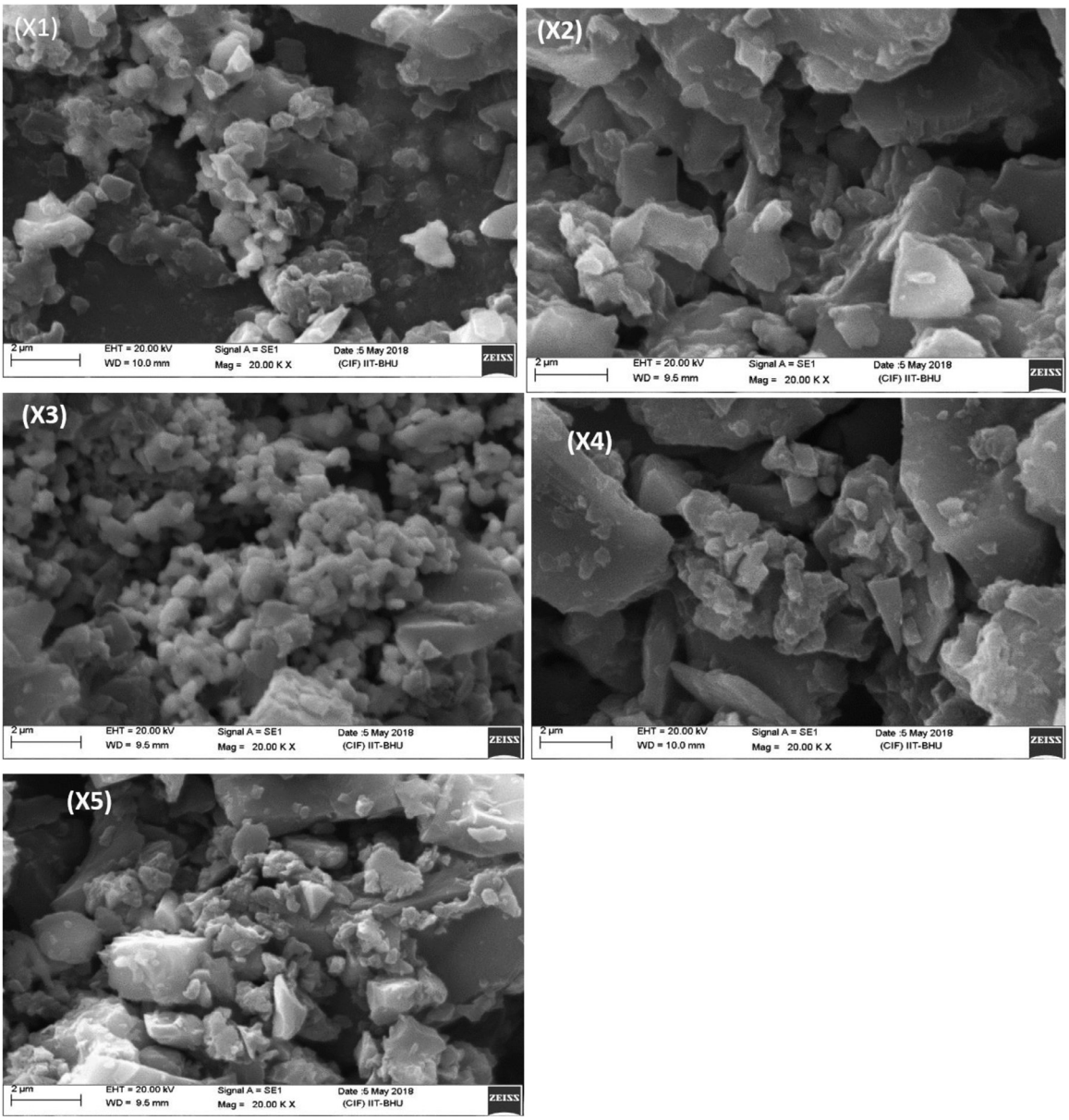

Fig. 2. SEM micrograph of different composition of porcelain material sintered at 1350 °C.

Table 1, was properly mixed evenly by agate mortar for 1 h and then further mixing were done through ball mill. For ball milling, ball mill jar was filled with the said composition (X1, X2, X3, X4 and X5) and grinding media of ZrO_2 balls and rotated on the ball mill machine for 6 h. Before the pellet formation process, 3–4 drops of 5% PVA binder was added in each powder sample and hand mixed thoroughly for 30 min [25–26].

The testing pellet samples were fabricated by using hydraulic press machine, prepared powder composition were compacted at 170 MPa.The method used for pellet formation was dying pressing. In this technique, the powder was compacted in carbon steel die of dia 15 mm and then is statically pressed further using hydraulic pressing machine. Pellets of different shape i.e. rectangular (40 mm x 10 mm x10mm) and circular (15 mm) were prepared for further physical and mechanical characterization. Solid state sintering technique is used for pellets fabrication, each prepared pellets having different compositions (X1, X2, X3, X4 and X5) sintered at 1250 °C and 1350 °C, using sintering rates of 5 °C/min with a soaking period of 2 h at the said peak temperature [27, 28].

2.1. Characterization

The sintered (1250 °C and 1350 °C) samples were used for different characterization, include scanning electron microscopy (SEM) and X ray difraction (XRD) analysis. For analysis the physical properties of the prepared composition were measured according to ASTM standards using hot water bath method.

Using the following data was collected regarding dry weight (D_w), Wet weight (W_w), and Suspended weight (S_w) for all types of samples,by using the formula

$$\text{Water absorption (W.A)} = \frac{W_w - D_w}{D_w} \times 100 \quad (1)$$

$$\text{Apparant Porosity (A.P)} = \frac{W_w - D_w}{w_w - S_w} \times 100 \quad (2)$$

$$\text{Bulk Density (B.D)} = \frac{D_w}{W_w - S_w}\text{gm/cm}^3 \quad (3)$$

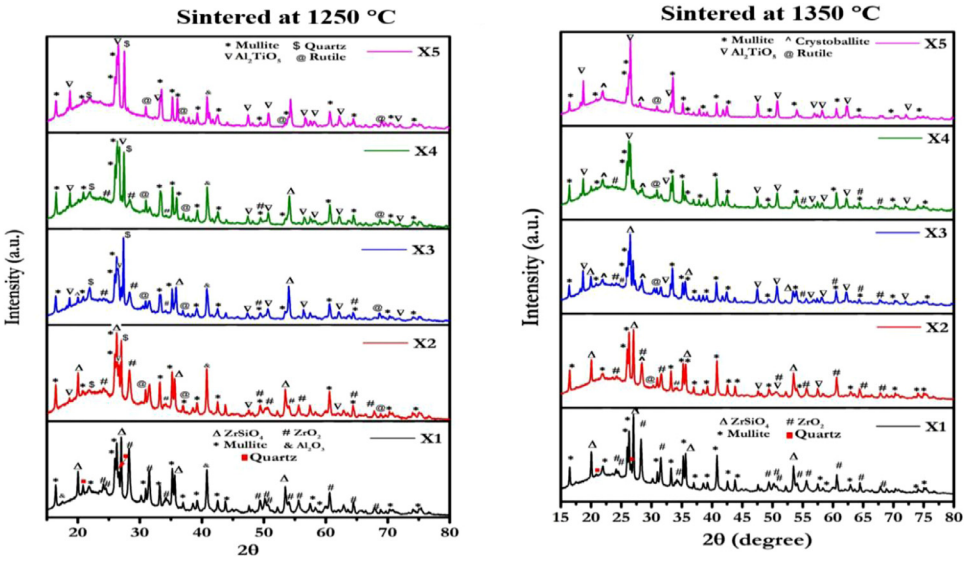

Fig. 3. XRD Analysis of porcelain composition sintered at different temperature (1250 °C and 1350 °C).

For linear shrinkage calculation, we are using the formula

$$\text{Linear shrinkage (L.S)} = \frac{L_i - L_f}{L_i} \times 100 \quad (4)$$

Where initial length without sintered (L_i) and final length after sintered (L_f)

The mechanical tests were carried out on Universal Testing Machine (UTM). The samples measurements were estimated and loaded in the software, then calculate the modulas of rapture or bending strength (B.S) and compressive strength of different prepared samples.For the analysis of B.S of the sample through UTM, three point bending test is performed.The sample is paced over two supporting pins kept a distance (L) apart and a third loading (F) pin is brought down from above at a constant rate until the failure of sample. A compression test can also be performed on UTM by placing the test sample on the base block. A compression testing machine consists of two pressure plates/heads. The upper head is movable while the lower head is fixed. One of the two heads is equipped with a hemispherical bearing to obtain uniform distribution of load on test-piece [29-30].

3. Result and discussion

The SEM micrographs of all the samples are shown below at magnifications of 20,000X. In the Fig. 1 it is clearly shown that the TiO_2 concentration of the sample increases, the particle density increases upto sample X3, and then the particle density starts decreasing, hence explaining the density variation. This also signifies that as TiO_2 content increases, the phase development is better. Also in 1350 °C samples, there are types of round crystals are formed which hints at the development of phases in the sample. The samples sintered at 1350 °C show more density than those of 1250 °C.The pores also decrease from X1 to X3 and then increase to X5. The pores in 1250 °C samples are more compared to the 1350 °C ones [31, 32].

The size range of all granular particles was varied between (0.6 to 3.6 μm) calculated by "Image J software" with varying degree of agglomeration. The particles present in samples were least agglomerated, high surface area and uniformly distributed. SEM image of Fig. 2 samples sintered at 1350 °C clearly showed that the Ti was finely dispersed over the metal. The quasi-spherical particles of various sizes were observed in the SEM images of all catalyst. The shape and homogeneity of the particles have changed with changing the composition of catalyst. The synergetic effect mainly depends upon the catalyst composition and nature of oxidized compounds. The phase identification and cell dimensions of samples were analysis by the X-ray powder diffraction (XRD) technique. It provides information about the structure, phase, crystal orientation, lattice parameters, crystallite size, strain and crystal defects etc. XRD analysis of all the samples was displayed in the Fig. 3. The powder samples were sintered and XRD analysis of each sample was carried out and peaks were analysed. The following points can be concluded:

1 The XRD analysis of all the samples were carried out and major phase of Mullite (JCPDS: 79–1453) was found in each sample.
2 Compounds with TiO_2 was found as Rutile(JCPDS: 73–2224) phase and Al_2TiO_5 (JCPDS: 70–1435). The peaks of these two phases increased from X2 to X5 sample signifying increase in Ti concentration and reaction of Al with TiO_2.
3 ZrO_2 was found as t-ZrO_2 (JCPDS: 36–0420) and as $ZrSiO_4$ (JCPDS: 80–1808). The peaks of these two phases increased from X4 to X1 sample signigying increase in Zr concentration and reaction of Si with ZrO_2.
4 In both 1250 °C and 1350 °C sintered samples, SiO_2 found as Quartz (JCPDS: 79–1906) has peaks decreasing from X1 up to X3 where they are minimal. Same pattern can be noticed in Al_2O_3 (JCPDS: 46–1212) where the peaks decreases from X5 to X3 where they are minimal. These two similar pattern suggests that the formation of most mullite in the sample X3.
5 In case of 1350 °C, the peaks of Quartz and Al_2O_3 were even lesser than their corresponding 1250 °C sintered samples suggesting more mullite formation at higher temperature.
6 Crystobalite (JCPDS: 39-1425) formed at 1350 °C increases thermal expansion coefficient and dielectric constant. $ZrSiO_4$ (JCPDS: 80-1808) and Al_2TiO_5 (JCPDS: 70-1435) promote the formation of mullite at even higher temperatures by its dissociation.

From Fig. 3, confirmed that the particles present in Al_2TiO_5/SiO_2 are most crystalline form and producing narrow size high-intensity diffraction lines; as compared to other samples. The crystallite size of particles present in the samples was analysis by the XRD technique was matched with the particle size calculated by the SEM characterization.

3.1. Physical analysis

From Fig. 4, confirm that the value of LS increase with sintering temperature during sintering all the inter particle spacing between the molecules become decreases result contraction in resultant volume of the materials. The results in physical parameters such as bulk density (B.D g/cm^3), apparent porosity (A.P in%), linear shrinkage (L.S in%), and water absorption (W.A with different sintering temperature are given in the Table 2 and shown in the Fig. 4.

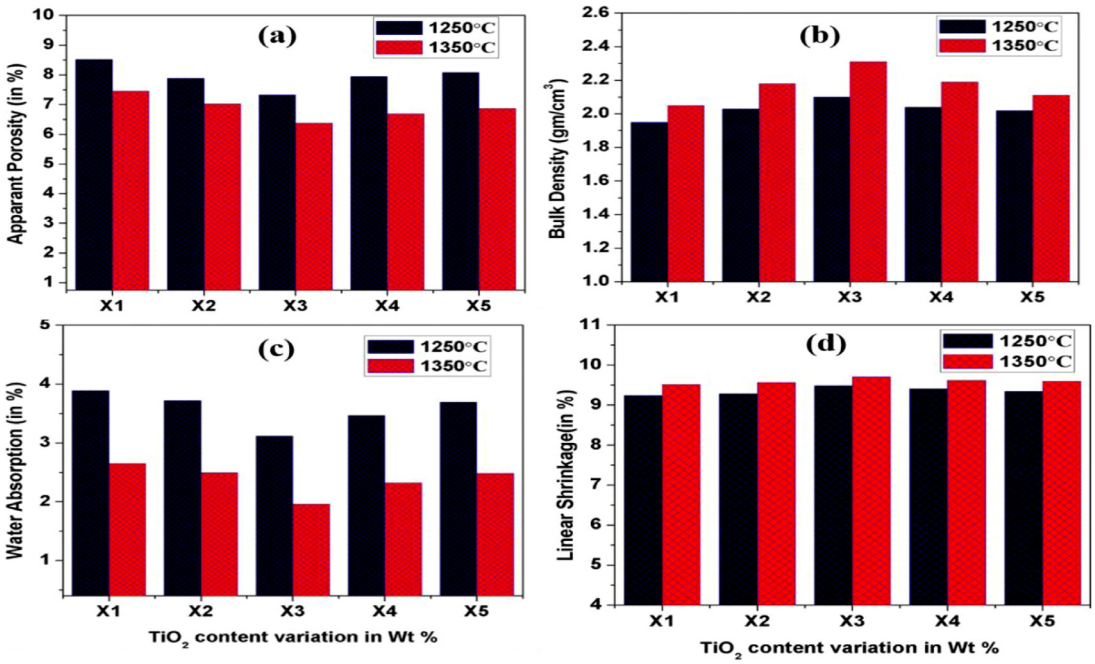

Fig. 4. Graph show relation between different physical parameters vs TiO_2 content (0–10%) of different samples composition sintered at 1250 and 1350 °C with soaking period for 2 h.

Table 2
Change in bulk density (B.D g/cc), apparent porosity (A.P%), linear shrinkage (L.S%), and water absorption (W.A) with different sintering temperature.

Temperature 1250 °C					
Samples	**X1**	**X2**	**X3**	**X4**	**X5**
B.D.	1.95	2.03	2.10	2.04	2.02
A.P in%	8.52	7.89	7.33	7.95	8.09
L.S in%	9.24	9.29	9.49	9.41	9.34
W.A.in%	3.89	3.72	3.12	3.47	3.69
Samples	**X1**	**X2**	**X3**	**X4**	**X5**
1350°C					
B.D.	2.05	2.18	2.31	2.19	2.11
A.P in%	7.45	7.03	6.37	6.69	6.87
L.S in%	9.52	9.57	9.71	9.62	9.60
W.A.in%	2.65	2.49	1.96	2.32	2.48

With sintering at two different temperatures (1250 °C and 1350 °C) the value of WA and AP were found to decrease with the addition of concentration of TiO_2 from 0 to 5 wt.% in the base composition of porcelain material. The WA of samples decreased with increasing sintering temperature because close pores and open porosities of the bodies reduced and there was increased glassy phase content in the samples. For sample X3, the value of WA and AP dropped to a minimum 1.96 and 6.37 respectively, by addition of 5 wt.% TiO_2 with 5 wt.% ZrO_2 for the sample sintered at 1350 °C with a soaking period of 2 h. Also recorded the maximum density of 2.31 g/cm^3 at the certain temperature for composition of sample X3.After the further addition of TiO_2 up to 10 wt.%, it starts to decrease because lack of glassy silica content, the proper bonding between Ti and Zr molecule become decreases and extra Ti content disperse on the surface of porcelain body results increases the closed pores due to that increase the water absorption in the resultant porcelain material, show in Fig. 4. Hence, the strength gradually decreases on further addition of TiO_2 for the X4 and X5 composition.

The mechanical tests were carried out on the Universal Testing Machine(UTM). The sample sizes were measured and fed in the software and bending and compressive strengths were calculated. For Modulus of Rupture (MOR) or Bending test calculation, a rectangular sample (40 mm × 10 mm × 10 mm) was using three-point bending test, and a cylindrical sample is having a dimension of 30 mm diameter was used for compressive strength measurement. The MOR is calculated using a formula:

$$\sigma_t = \frac{3FL}{2wt^2} \tag{5}$$

Where, F is force in Newton at which the sample is fails, L is the length between supports, W is width, and t is thickness of the sample

From the Fig. 5, as the TiO_2 content increases and ZrO_2 content decreases upto 5 wt.% the strength of samples X1, X2 and X3 increases and then decreases afterwards for the sample X4 and X5. The maximum mechanical strength is recorded for the sample X3 having bending strength (96.28± 5 MPa) and compressive strength (158.71± 5 MPa), respectively, shown in the Fig. 5. The decrease in strength for sample X4 and X5 is due to increase in porosity and density goes down which is shown in the Fig. 5. Also, in accordance to the XRD analysis, which shows that the presence of mullite phase in sample X3. However as the ZrO_2 content decreases subsequently alongwith less mullite phase development, the bending strength decreases. The compressive strength showed higher values than that of bending strength, due to the difference in stresses distribution during compression of the samples.

4. Conclusion

In this work, mechanically strong porcelain insulating materials were prepared using low-cost clay composition and varying concentration of zirconia and TiO_2. The effect of sintering temperature and TiO_2 wt.% was studied. The base composition having concentration of 5 wt.% ZrO_2 and 5% wt. TiO_2 sintered at 1350 °C (X3) found to be most suitable in refractory and high-temperature applications where severe thermal shock with high mechanical features are required. In the composition with increasing sintering temperature the phase reactions occur at their best and give the desired phases, the ceramic particles tend closer to each other and lead to densification up to 2.1 g/cc at 1350 °C. Result reduction in porosity due to lack of close pores. The non-availability of micro cracks and pores, reduction in porosity due to reduction in

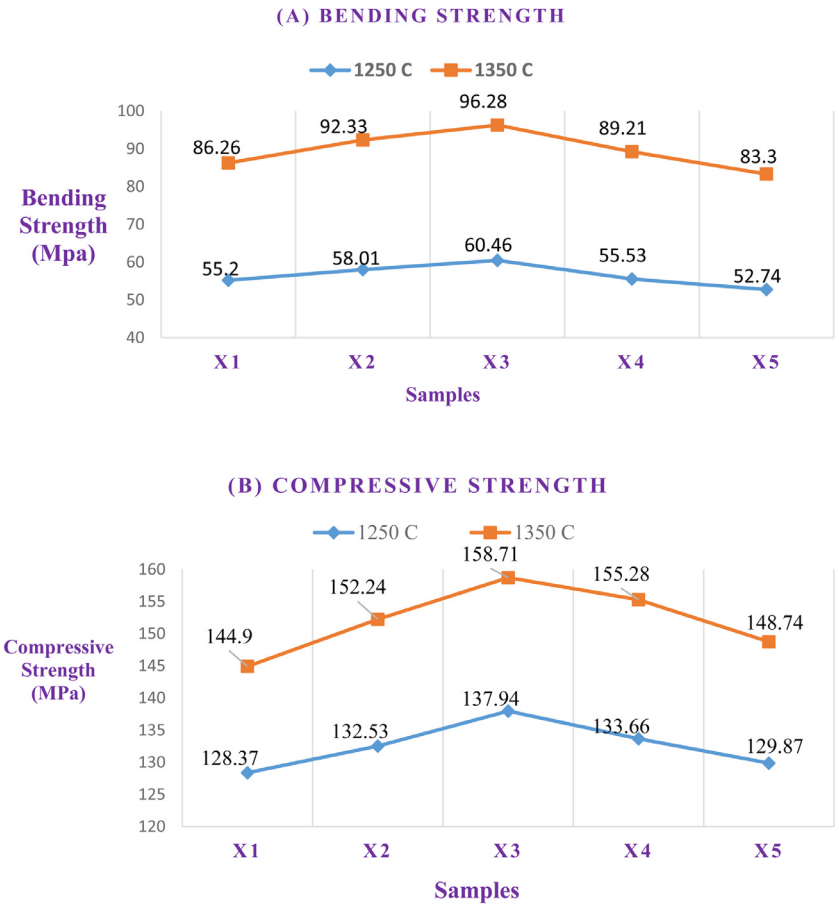

Fig. 5. Graph show relation between mechanical behavior vs TiO_2 content (0–10%) sintered at 1250 and 1350 °C i.e. (A) Bending strength and (B) Compressive strength.

water absorption of the resultant porcelain composition . The recorded value of bending strength and compressive strength was 96.28 MPa and 158.71 MPa respectively at 1350 °C. On further addition of TiO_2 up to 10 wt.%, the strength of resultant porcelain material gradually starts to decrease due to lacks of glassy phase content and bonding between Ti and Zr become decreases results increases the closed pores.

Declaration of Competing Interest

The authors declare that they have no known competing financial interests or personal relationships that could have appeared to influence the work reported in this paper.

References

[1] R.C. Buchanan, Properties of ceramic insulators, in: R.C. Buchanan (Ed.), Ceramic Materials for Electronics, 2nd ed., Marcel Dekker Inc., Ed. New York, 1991, pp. 1–67.
[2] K. Dana, S. Das, K.S. Das, Effect of substitution of fly ash for quartz in triaxial kaolin-quartz-feldspar system, J. Eur. Ceram. Soc. 24 (2004) 3169–3175.
[3] P.W. Olupot, S. Jonsson, J.K. Byaruhanga, Study of glazes and their effects on properties of triaxial electrical porcelains from Ugandan minerals, J. Mater. Eng. Perform. 19 (8) (2010) 1133–1142.
[4] P.W. Olupot, Assessment of ceramic raw materials in Uganda for electrical porcelain, Peter Wilberforce Olupot, Licentiate Thesis in Material Science Department of Materials Science and Engineering Royal Institute of Technology (KTH), 2006 Stockholm, Sweden.
[5] S. Kasrani, A. Harabi, S.E. Barama, L. Foughali, M.T. Benhassine, D.M. Aldhayan, Sintering and dielectric properties of a technical porcelain prepared from economical natural raw materials, Cerâmica 62 (364) (2016) 405–412.
[6] M. Touzin, D. Goeuriot, C. Guerret-Piécourt, D. Juvé, H.J. Fitting, Alumina based ceramics for high-voltage insulation, J. Eur. Ceram. Soc. 30 (4) (2010) 805–817, doi:10.1016/j. jeurceramsoc.2009.09.025.
[7] S.R. Bragança, C.P. Bergmann, A view of white wares mechanical strength and microstructure, Ceram. Int. 29 (2003) 801–806.
[8] O.I. Ece, Z. Nakagawa, Bending strength of porcelains, Ceram. Int. 28 (2002) 131–140.
[9] M. Romero, J.M. Pérez, Relation between the microstructure and technological properties of porcelain stoneware. A review, Mater. Construct. 65 (2) (2015) 1–19.
[10] P.K. Sahu, L. Chandra, R.K. Pandey, N.S. Mehta, R. Dwivedi, V.N. Mishra, R. Prakash, Fast development of self-assembled, highly oriented polymer thin film and observation of dual sensing behavior of thin film transistor for ammonia vapor, Macromol. Chem. Phys. 220 (2019) 1900010, doi:10.1002/macp.201900010.
[11] N.S. Mehta, M.R. Majhi, Effect of sintering at different temperature to enhance the physical and mechanical properties of forsterite refractories doped, Int. J. Innovat. Res. Sci. Eng. Technol. (2016) 16261–16266, doi:10.15680/IJIRSET.2016.0509086.
[12] F.A. Andrade, H.A. Al-Qureshi, D. Hotza, Measuring the plasticity of clays: a review, Appl. Clay Sci. 51 (1–2) (2011) 1–7, doi:10.1016/j.clay.2010.10.028.
[13] N.S. Mehta, S. Dey, M.R. Majhi, Electro-mechanical characterization of alumina-based porcelain insulator doped with $BaTiO_3$ at high temperature with frequency variation, Mater. Chem. Phys. 259 (2021) 124020.
[14] C. Ancey, Plasticity and geophysical flows: a review, J. Nonnewton. Fluid Mech. 142 (1–3) (2007) 4–35, doi:10.1016/j.jnnfm.2006.05.005.
[15] N.S. Mehta, P.K. Sahu, P. Tripathi, R. Pyare, M.R. Majhi, Influence of alumina and silica addition on the physico-mechanical and dielectric behavior of ceramic porcelain insulator at high sintering temperature, Boletín la Soc. Española Cerámica y Vidr. (2017) 1–9, doi:10.1016/j.bsecv.2017.11.002.
[16] J.E. Contreras, E.A. Rodríguez, Nanostructured insulators – A review of nanotechnology concepts for outdoor ceramic insulators, Ceram. Int. 43 (12) (2017) 8545–8550.
[17] N. Panday, I. chakrabarty, K. Bakane, N.S. Mehta, M.R. Majhi, Microstructure, mechanical and wear properties of aluminum borate whisker reinforced aluminum matrix composites, Transec. Nonferrous Metal. Allow Soc. 30 (2020).
[18] G. Gralik, A.L. Chinelatto, A.S.A. Chinelatto, Effect of different sources of alumina on the microstructure and mechanical properties of the triaxial porcelain, Ceramica 60 (356) (2014) 471–481.
[19] R. Krishnan, S. Samanta, R. Sudha, K. Govardhan, Electric field analysis of high voltage insulators, Int. J. Comput. Informat. 1 (4) (2012) 31–35.
[20] P. Ramaswamy, S. Vynatheya, S. Seetharamu, Significance of structure-property relationship in alumina based porcelain insulators to achieve quality, Bull. Mater. Sci. 28 (7) (2005) 681–688.
[21] S.S. Owoeye, T.S. Toludare, O.E. Isinkaye, U. Kingsley, Influence of waste glasses on the physico-mechanical behavior of porcelain ceramics, J. Span. *Ceram.* Glass *Soc.* 58 (2) (2019) 77–84.
[22] R.A. Islam, Y.C. Chan, M.F. Islam, Structure-property relationship in high-tension ceramic insulator fired at high temperature, Mater. Sci. Eng.: B 106 (2) (2004) 132–140, doi:10.1016/j.mseb.2003.09.005.

[23] W. Lerdprom, C. Li, D.D. Jayaseelan, S.J. Skinner, W.E. Lee, Temperature dependence of electrical conductivity of a green porcelain mixture, J. Eur. Ceram. Soc. 37 (1) (2017) 343–349, doi:10.1016/j.jeurceramsoc.2016.08.019.

[24] N. Montoya, F.J. Serrano, M.M. Reventós, J.M. Amigo, J. Alarcón, Effect of TiO_2 on the mullite formation and mechanical properties of alumina porcelain, J Eur Ceram Soc 30 (4) (2010) 839–846, doi:10.1016/j.jeurceramsoc.2009.10.009.

[25] S. Dey, N.S. Mehta, Synthesis and applications of titanium oxide catalysts for lower temperature CO oxidation, Current Res. Green Sustain. Chem. 3 (2020).

[26] N.S. Mehta, J.C. Pandey, N. Pandey, R. Pyare, M.R. Majhi, Developing a high strength physico-mechanical and electrical properties of ceramic porcelain insulator using zirconia as an additive Developing a high strength physico-mechanical and electrical properties of ceramic porcelain insulator using zirconia as an additive, Mater. Res. Express 5 (7) (2018) 75202.

[27] Y. Zheng, X. Wang, G. Wu, Chemical modification of carbon fiber with diethylenetriamine pentaacetic acid/halloysite nanotube as a multifunctional interfacial reinforcement for silicone resin composites, Polym. Adv. Technol. 31 (3) (2019) 527–535.

[28] Y. Zheng, L. Chen, X. Wang, G. Wu, Modification of renewable cardanol onto carbon fiber for the improved interfacial properties of advanced polymer composites, Polymers (Basel) 12 (1) (2019) 45, doi:10.3390/polym12010045.

[29] Q. Wang, H. Li, X. Yu, Y. Jia, Y. Chang, S. Gao, Morphology regulated Bi_2WO_6 nanoparticles on TiO_2 nanotubes by solvo thermal Sb^{3+} doping as effective photocatalysts for wastewater treatment, Electrochim. Acta 330 (2020) 135167.

[30] D. Cao, Q. Wang, Y. Wu, S. Zhu, Y. Jia, R. Wang, Solvothermal synthesis and enhanced photocatalytic hydrogen production of Bi/Bi_2MoO_6 co-sensitized TiO_2 nanotube arrays, Sep. Purif. Technol. 250 (2020) 117132.

[31] A. Sedghi, N. Hamidnezhad, N.R. Noori, The effect of fluxes on alumina silicate porcelain insulator properties and structure, in: Proceedings of the International Conference on Ecological, Environmental and Biological Sciences (ICEEBS'2012), 7, 2012, pp. 343–345.

[32] N.S. Mehta, P.K. Sahu, M.R.Majhi Saxena, M. Ershad, R. Pyare, Effect of ZrO_2 on the sintering behavior, strength and high-frequency dielectric properties of electrical ceramic porcelain insulator, Mater. Res. Express 5 (1) (2018) 015202, doi:10.1088/2053-1591/aaa5b9.